Available online at www.sciencedirect.com

ScienceDirect

Current Opinion in Structural Biology

Rotary ATPases — dynamic molecular machines

Alastair G Stewart[1,2], Elise M Laming[1,2], Meghna Sobti[1,2] and Daniela Stock[1,2]

Recent work has provided the detailed overall architecture and subunit composition of three subtypes of rotary ATPases. Composite models of F-type, V-type and A-type ATPases have been constructed by fitting high-resolution X-ray structures of individual components into electron microscopy derived envelopes of the intact enzymes. Electron cryo-tomography has provided new insights into the supra-molecular arrangement of eukaryotic ATP synthases within mitochondria. An inherent flexibility in rotary ATPases observed by different techniques suggests greater dynamics during operation than previously envisioned. The concerted movement of subunits within the complex might provide means of regulation and information transfer between distant parts of rotary ATPases thereby fine tuning these molecular machines to their cellular environment, while optimizing their efficiency.

Addresses
[1] The Victor Chang Cardiac Research Institute, Sydney, NSW, Australia
[2] The University of New South Wales, Sydney, NSW, Australia

Corresponding author: Stewart, Alastair G (a.stewart@victorchang.edu.au)

Current Opinion in Structural Biology 2014, **25**:40–48

This review comes from a themed issue on **Macromolecular machines**

Edited by **Karl-Peter Hopfner** and **Tom Smith**

For a complete overview see the Issue and the Editorial

Available online 21st December 2013

0959-440X

http://dx.doi.org/10.1016/j.sbi.2013.11.013

Introduction

Rotary ATPases are molecular motors that couple ATP turnover with ion translocation through membranes and are central to biological energy conversion as well as being integral to the acidification of intracellular compartments [1–3]. They are found across all known forms of life and, while they share similar overall architectures, they can be classified into several sub-types depending on their cellular function and taxonomic origin (Figure 1).

Eukaryotes contain both ATP synthases (F-type) [4] and vacuolar ATPases (V-type) [3] that are specialized in opposite functions (Figure 1a,b). F-type ATP synthases are found within mitochondria or chloroplasts where they act as biological power converters [2]. Utilizing the potential energy from transmembrane electrochemical proton gradients generated by photosynthesis or respiration, they synthesize the biological energy carrier, adenosine triphosphate (ATP) in an endergonic reaction. V-type ATPases on the other hand are biological rotary pumps that use energy derived from ATP hydrolysis to pump ions across membranes, thereby building up electrochemical potential gradients used as energy sources for secondary transport [3]. Most bacteria contain only one type of rotary ATPase, either a bacterial F-type ATPase/synthase (Figure 1c) or a bacterial A/V-type ATPase/synthase (Figure 1d), and these are believed to be bifunctional [5,6]. The same is true for archaea that contain an A-type ATPase/synthase [7] (Figure 1d) that is closely related to the bacterial A/V-type enzymes and, to a lesser extent, to eukaryotic V-type ATPases.

All types of rotary ATPases contain two motors, R_1 and R_O, that are coupled with one another, one motor being able to drive the other [8]. This is achieved by connecting each motor with central and peripheral stalks (Figure 1). The soluble R_1 motors contain three nucleotide-binding sites for ATP turnover, whereas the R_O motors are membrane bound and translocate protons or other cations.

Rotary ATPases can be thought of as being made up of 'machine elements', comparable to those of man-made engines [1,9]. ATP synthases work analogously to a hydroelectric generator, where water from a storage reservoir has the propensity to flow down hill (gravitational potential), thereby generating torque in turbines that is converted into electricity. Protons likewise have the potential to flow from high to low concentration (electrochemical potential, also called 'proton motive force' or pmf) thereby generating torque in R_O. To translocate through the membrane, protons are believed to bind sequentially to subunits of a ring, which rotates within the membrane. This biological turbine is attached to a central stalk that enables mechanical energy to be transferred between each motor, analogous to the way a crankshaft transfers torque. Indeed the central stalk is curved like a crank and pushes catalytic subunits in R_1 into different conformations to provide the correct chemical environment for ATP synthesis from its building blocks, ADP and inorganic phosphate, P_i.

Figure 1

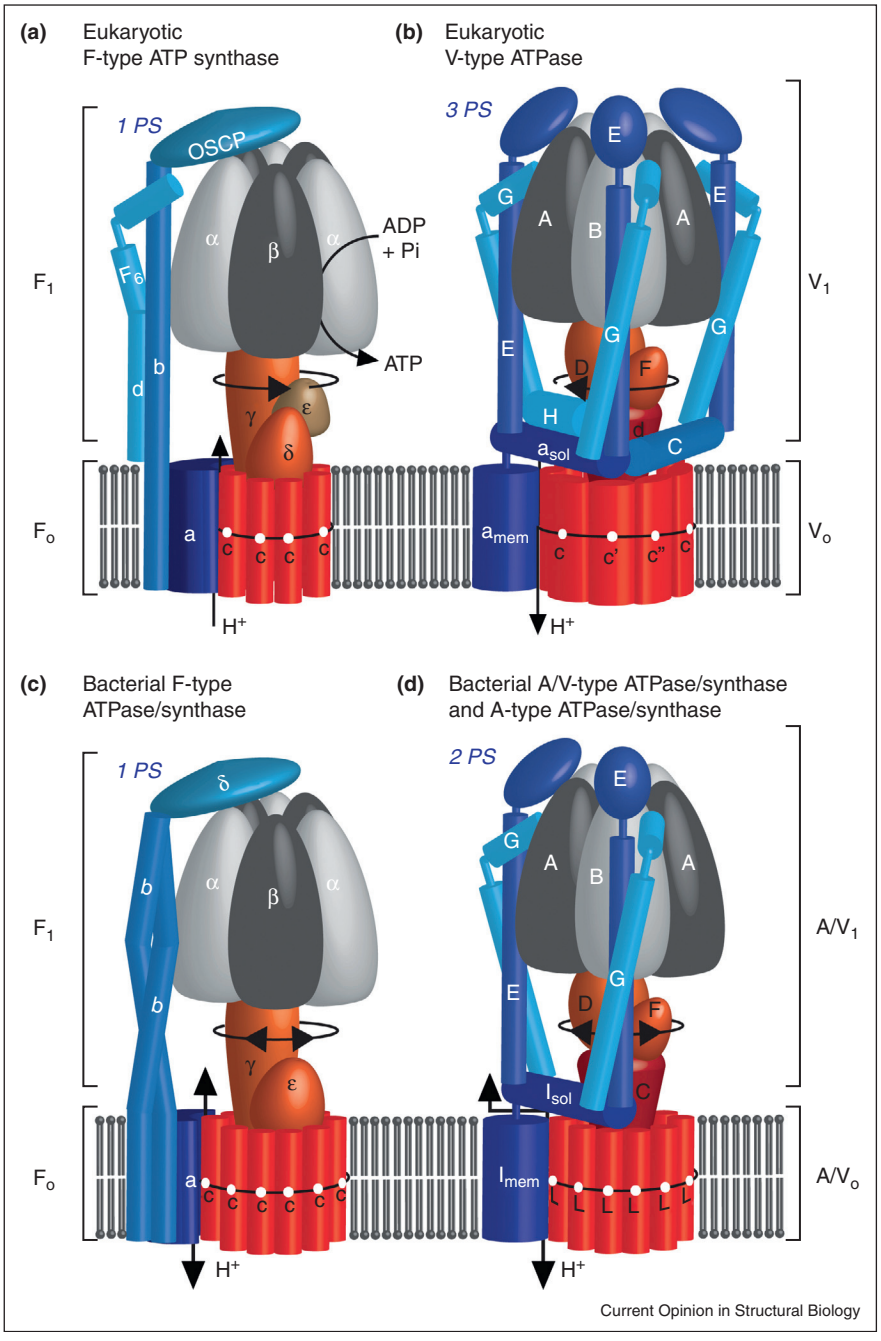

Schematic diagrams of rotary ATPase subtypes and their major subunits. **(a)** Eukaryotic mitochondrial F-type ATP synthase (containing one peripheral stalk, PS) synthesizes ATP using energy derived from a transmembrane proton gradient generated by respiration. **(b)** Eukaryotic V-type ATPases (containing three PS) are situated in intracellular membranes using energy from ATP hydrolysis to pump protons across membranes. **(c)** Bacterial F-type ATPases/synthases (containing one PS) synthesize ATP, but can revert and act as proton pumps if ATP levels are high. **(d)** Bacterial V-type and archaeal A-type ATPases share the same architecture and contain two peripheral stalks. Like bacterial F-type ATPases they are believed to be bi-functional. Nucleotide binding subunits are shown in greys, other stator subunits in blues, rotor subunits in reds and protons as white spheres.

In the reverse reaction (ATPase), the R_1 motor works in much the same way as an internal combustion engine. The pseudo-threefold ATPase engine sequentially provides different chemical environments for ATP binding (fuel intake), followed by hydrolysis (power-stroke), and final release of the products, ADP and P_i (exhaust gas release), so ATP can be bound again [2,4,10]. The peripheral stalk(s) act as stators and hold the two motors

Figure 2

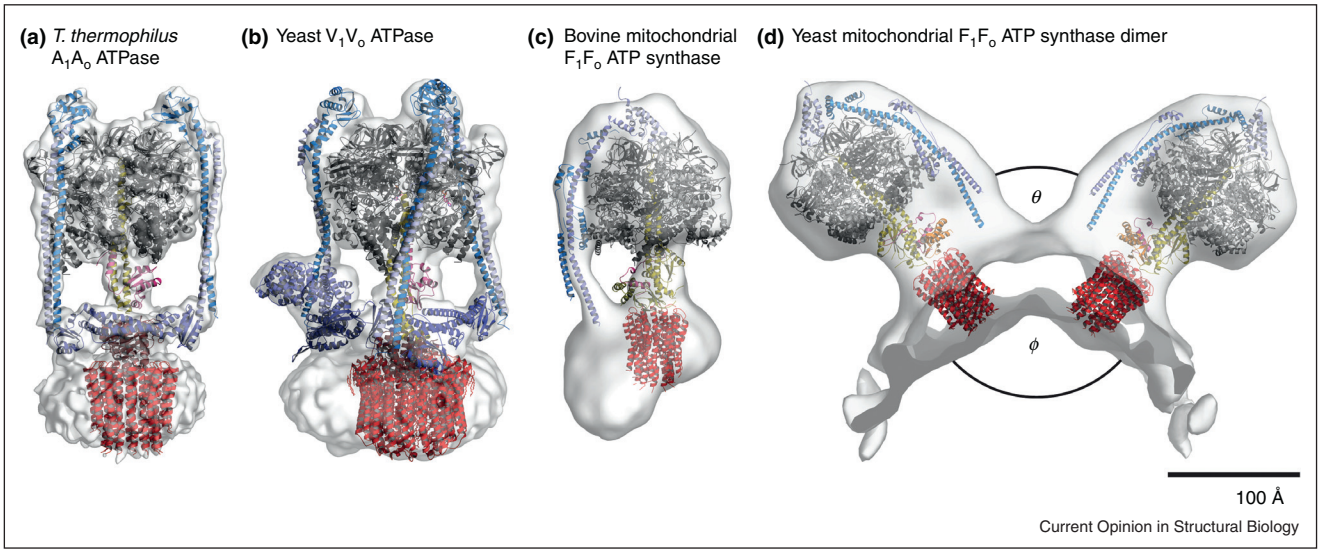

Composite models of rotary ATPases derived from fitting X-ray structures into EM densities. **(a)** *T. thermophilus* bacterial A/V-type ATPase/synthase (EMD: 5335 [14••] and pdbs: 3j0j [14••], 3rrk [54] and 1c17 [55]). **(b)** Yeast V-type ATPase (EMD: 5476 [15•] and pdbs: 3a5c, 3aon, 1r5z, 2bl2, 4dl0, 3rrk, 1u7l and 1ho8 [1]). **(c)** Bovine mitochondrial F-type ATP synthase (EMD: 2091 [16•] and pdb: 4b2q [11••]). **(d)** Yeast mitochondrial F-type ATP synthase dimer (EMD: 2161 and pdb: 4b2q [11••]), angles between ATP synthase dimers and cristae shown as θ and ϕ respectively. Color scheme as in Figure 1.

relative to one another so that the energy can be transferred. Without this key component, no torque would be transferred, as the catalytic subunits would simply follow the rotation of the crankshaft.

Over the past two years, a wealth of new insights has come from a range of complementary techniques; electron cryotomography (ECT) has provided low-resolution pictures of mitochondrial ATP synthases *in situ* [11••,12••,13•], while cryo-electron microscopy (cryo-EM) reconstructions of all three types of rotary ATPases have reached nanometre resolution [14••,15•,16•]. These reconstructions have not only provided envelopes describing the overall architecture of the motors, but in the case of the *Thermus thermophilus* A/V-ATPase/synthase (*Tt*ATPase), has also shown what could possibly be evidence of the proton path through the membrane [14••]. Detail to atomic resolution of the peripheral stalks has provided insight into their function and dynamics within the rotary ATPase during operation [17,18••,19•,20].

Overall architecture of rotary ATPases — a new level of detail and a first glimpse of the proton path

Advances in electron microscopy methods and analysis have provided 3D EM reconstructions of all three classes of rotary ATPases at or near the nanometer scale [14••,15•,16•]. The reconstructions provide a detailed envelope into which atomic resolution crystal structures can be fitted, providing composite models of the intact complexes (Figure 2).

The reconstruction of the *Tt*ATPase to 9.7 Å resolution [14••] (Figure 2a) has yielded the greatest detail of any intact rotary ATPase to date, providing enough structural detail to suggest that the two half channel model of proton translocation proposed by Junge and Vik is correct [21,22]. In this model, a ring of subunits (termed proteolipids) within the R_O motor carries out rotational diffusion relative to the stator by sequentially binding protons [23] (Figure 3a). An essential and universally conserved acidic residue on each subunit must be deprotonated when facing a positive residue on the stator, but must be protonated when facing the hydrophobic lipidic membrane [24,25]. It is believed that there are two non-collinear 'half' channels for protons from either aqueous phase leading to the acidic residue on the ring. The positive residue on the stator prevents short-circuiting of the proton flow, as well as giving directionality to the motor by attracting the opposing negative charge. The high-resolution reconstruction of the *Tt*ATPase provides structural evidence that the proteolipid ring is exposed to the solvent on either side of the ring, although there is insufficient detail yet to visualize the exact proton path (Figure 3b).

In the reconstruction, eight transmembrane helices can be resolved for the stator subunit as previously predicted [26], and 24 for the 12 proteolipid subunits. The stator subunit helices divide into two bundles, each containing four helices (Figure 3b). One bundle appears almost perpendicular to the membrane and contacts a single proteolipid near the middle of the membrane. The other bundle appears tilted and contacts the adjacent

Figure 3

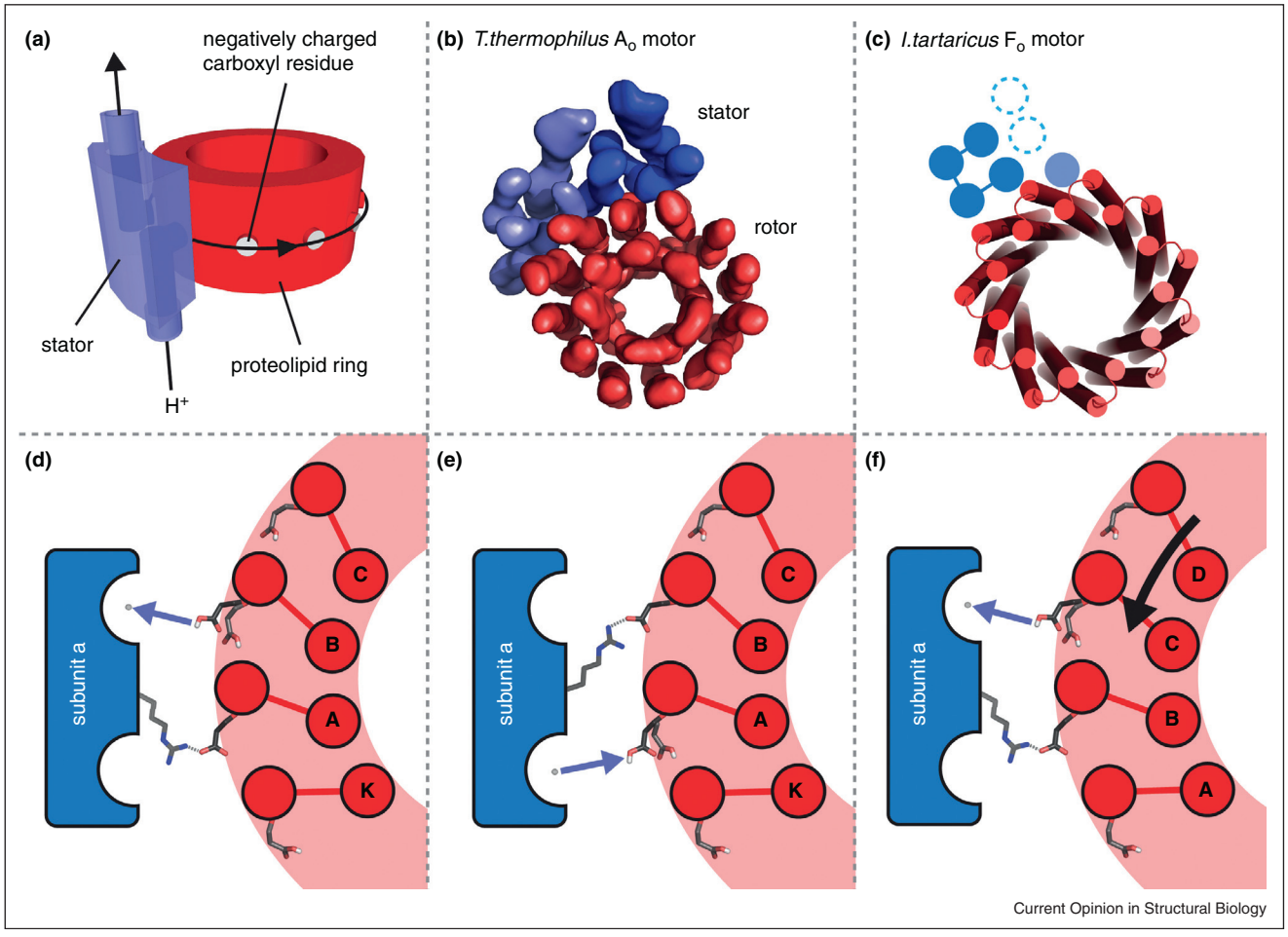

The R_O motor and models for the generation of rotation, with the proteolipid ring in red and the R_O stator subunit in blue. **(a)** Schematic model of the 'two half-channel' hypothesis (adapted from [56]). **(b)** A_O portion of the *T. thermophilus* bacterial A/V-type ATPase/synthase (EMD: 5335 [14••]), with the R_O stator subunit four helix bundles shown in light and dark blue. **(c)** Schematic model of the F_O motor 2D EM density (adapted from [27•]). (d, e and f) Specific sequence of steps in the proposed mechanism; **(d)** opening and deprotonation, **(e)** rearrangement of Glu-Arg ion pair and reprotonation, **(f)** rotation (adapted from [28]).

proteolipid closer to the periplasm. This arrangement places the two proteolipids in distinct chemical environments and establishes the conditions necessary for a two half-channel model of proton translocation.

Cryo-electron crystallography of 2D crystals of the *Ilyobacter tartaricus* F_O complex yielded a projection map at a resolution of 7.0 Å [27•]. In contrast to the eight transmembrane helices found in the A_O stator, only seven transmembrane helices were observed in F_O (Figure 3c). However, four of these helices form a bundle, reminiscent of that found in the A_O counterpart, suggesting at least some similarity in function between the two subtypes. To the side of this bundle, a fifth helix contacts the proteolipid ring and two other helices can be resolved, albeit weakly. Thus, despite an arguably conserved ion translocation mechanism in different rotary ATPase subtypes [28,29], the rotor–stator interface architecture appears to vary.

The work on the proton path has been supplemented by multiple crystal structures of proteolipid rings from a range of organisms [28–31], which have provided atomic detail of how the ions bind to specific residues in the ring. Dicyclohexylcarbodiimide (DCCD) specifically inhibits ATPase activity and proton translocation by reacting with the conserved acidic residues of the rotor ring. In the crystal structures of the *Spirulina platensis* and *Enterococcus hirae* rotor rings, DCCD binds Glu62 and Glu139 respectively [28,29]. By controlling the pH during crystallization of the *S. platensis* and *Saccharomyces cerevisiae* rings [31], the authors were able to show that the glutamate adopts

an alternate rotamer depending on whether the residue is protonated or not (Figure 3d–f).

In addition to structural studies of the isolated rotor ring, mass spectrometry has been employed to identify membrane lipids associated with the native intact complex [32••,33•]. The rotor ring was found to bind specific lipids that do not represent the predominant lipid species found in the host membrane, suggesting that they are selected *via* high affinity binding to R_O. The function of these lipids is still unknown; however they may fill gaps in the protein surface to facilitate smooth rotation within the membrane as well as sealing to prevent proton leaks in analogy to the functions of machine oil [1,32••].

ATP synthase dimers — complexes of life and death

ECT of intact mitochondria has shown that mitochondrial cristae are shaped by lines of dimers of ATP synthases [11••,34] (Figure 2d). Moreover, other respiratory complexes appear to be located in close proximity to the ATP synthase, forming supercomplexes [12••,35,36]. Placing these respiratory complexes near the vertices of the cristae generates the proton gradient next to where it is needed while the vertices themselves might enhance the steepness of the gradient (see [37] for an explanation). Interestingly, the angle between the ATP synthase complexes within the dimers (reminiscent of the angle between rows of cylinders in a V-type car engine) has been shown to vary depending on species [12••], ranging from $\sim 80^\circ$ in bovine mitochondria to $\sim 115^\circ$ in potato. A larger angle, θ, between ATP synthase dimers will lead to a narrower cristae angle, ϕ (Figure 2d). This will increase the steepness of the electrochemical potential gradient across the membrane [37], which in turn might be an explanation for the different proton to ATP ratios found in different species. Although all R_1 motors turn over three ATP molecules per 360° cycle, the number of proton translocating subunits in R_O has been shown to vary between species with eight subunits in bovine mitochondria [38], 10 in yeast mitochondria [39] and up to 15 in cyanobacteria [40]. Similar to the relative number of teeth in a gear, a larger number will make the R_O motor stronger and more difficult to reverse (as it is proton driven), while a smaller number will lead to an earlier stall and to the R_1 motor dominating (as it is ATP driven) [1,2,41,42]. A larger θ angle however, will increase the potential energy of each proton, resulting in such ATP synthases operating with a smaller proton to ATP ratio, like those observed in mammalian mitochondrial ATP synthases [38].

As well as shaping the cristae, the dimerization of ATP synthase has recently been shown to be important in cell ageing and death. By observing the mitochondria of an organism as it ages, it has been shown that the ATP synthase dimers appear to dissociate from one another leading to the collapse of cristae, rupture of the mitochondria and eventually death of the cell [13•]. And on a related note, the mitochondrial permeability transition pore, a key effector of cell death, has been suggested to be formed from dimers of ATP synthase [43•].

The peripheral stalks — more than mere scaffolds

To prevent rotation between the stationary parts of the R_1 and R_O motors, the two motors need to be connected by one or multiple peripheral stalks. However, recent studies have highlighted that these domains may perform more than just a structural role and atomic detail of the complexes has uncovered a unique protein fold that facilitates its functions.

Two crystal structures of the peripheral stalk from *Tt*ATPase, PS1 and PS2, have been solved in different crystal forms to 3.1 Å [17] and 2.25 Å [18••] resolution. These show an elongated heterodimeric complex that contains two distinct domains; a 140 Å long coiled coil and a globular head (Figure 4a,b). Fitting of this complex into the 3D reconstruction of the intact complex showed that the globular head attaches to the A_1 motor and the coiled coil spans the gap between the motors, attaching to the A_O stator subunit (Figure 4c). The coiled coil domain is unusual, in that it coils in a right-handed manner rather than the common left-handed one. This arrangement results in almost parallel helices in the region that spans the space between the A_O and A_1 motors. A consequence of having almost parallel helices is that the peripheral stalk coiled coil is more flexible in the direction that it is thinnest (the *y* direction in Figure 4d), owing to the flexibility being proportional to the cross-sectional area. This is intriguing with regard to the intact complex, as the parallel helices are aligned such that they are most rigid in the direction of rotation (Figure 4c,e), consistent with this rare protein fold having evolved to provide the greatest rigidity in opposing the torque within the intact enzyme, while it is flexible in the perpendicular direction to accommodate conformational changes in the nucleotide binding subunits [18••].

The flexibility of the parallel helices can be seen when the two crystal structures are compared to one another (Figure 4a,b), again showing flection in the thinnest direction. The two conformations observed are related to one another by their two lowest energy normal modes. The ability of the complex to flex in such a manner may allow the stalks to follow movements of the catalytic subunits during the rotary catalytic cycle, preventing the need to break and re-form chemical bonds that hold the complex together thereby optimizing efficiency. In addition, the concerted movement of subunits may provide a means of information transfer between distant parts.

Figure 4

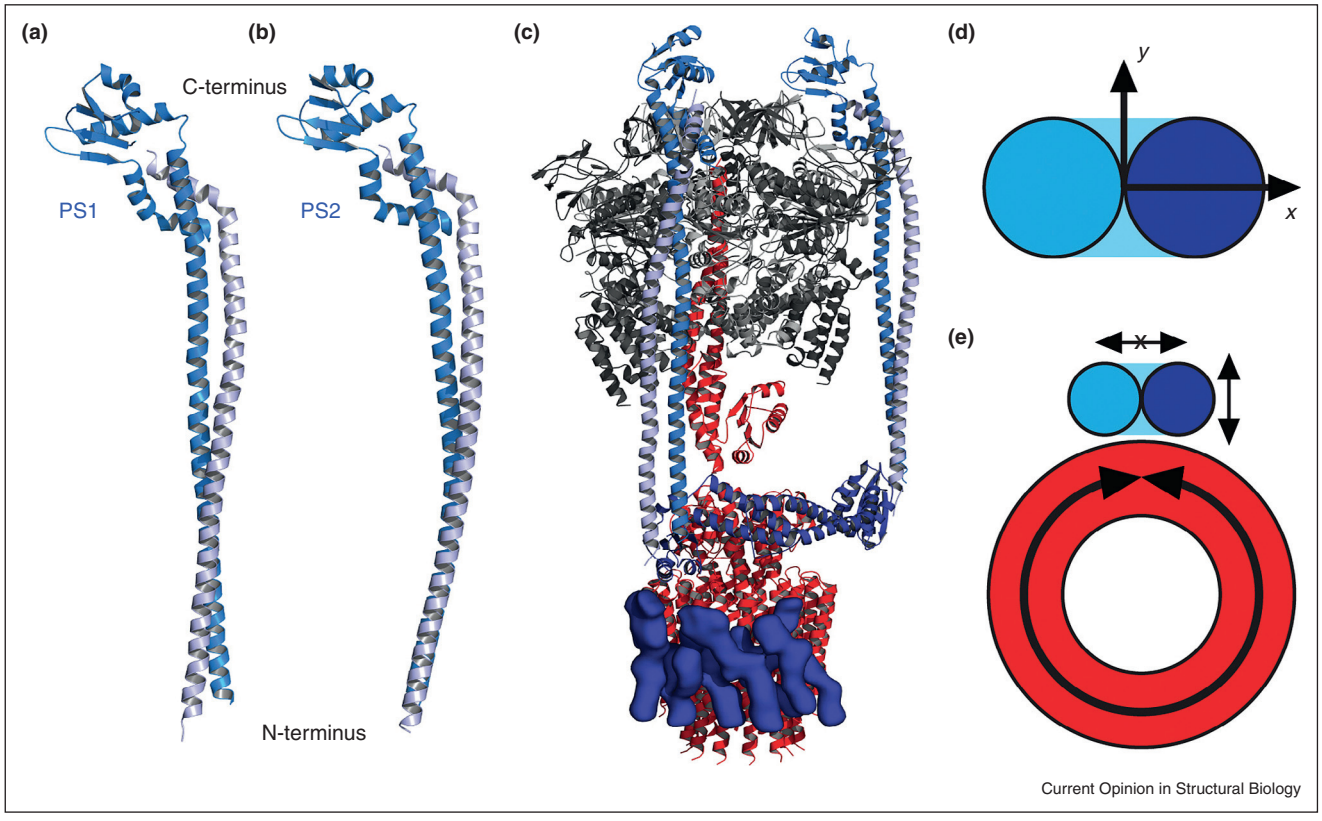

Peripheral stalk structures and their bending properties. **(a)** and **(b)** Crystal structures of the peripheral stalk from *T. thermophilus* bacterial A/V-type ATPase/synthase, pdb 3k5b [17] and 3v6i [18••] respectively. **(c)** Composite model of the intact *T. thermophilus* bacterial A/V-type ATPase/synthase using same colors as Figure 1. **(d)** Cross-section of two parallel helices on Cartesian co-ordinates, the cross-sectional area is smaller in the y direction, resulting in greater flexibility. **(e)** Schematic diagram showing how the parallel helices of the peripheral stalks are positioned to provide greatest rigidity in the direction of rotation.

Crystal structures of the yeast V-type peripheral stalk complex have also been solved in two different conformations that likewise show a bending over the length of the right-handed coiled coil [19•]. In contrast to the *Tt*ATPase peripheral stalk this is accentuated by 'skips' in periodicity of the right-handed coiled coil sequence repeats and a short random coil 'bulge' just below the globular head adding greater flexibility to these regions. Fitting of both structures into 3D EM reconstructions of the intact eukaryotic V-ATPase [44] indicates that significant bending must occur during assembly of the complex. Taken together, this suggests a possible 'spring-loading' mechanism during assembly of the eukaryotic V-ATPase complex, which puts the intact complex under strain so that it is primed to disassemble when signalled to do so. The spring-loading mechanism is supported by the observation that the assembly of eukaryotic V-ATPases requires the protein RAVE, suggesting that this chaperone may provide the energy needed to incorporate the peripheral stalks into the V-ATPase in a strained conformation. However, recent EM studies of the isolated V_1 motor from *Manduca sexta* show little structural rearrangement when compared to the activated complex [45,46], leaving this matter unresolved.

Lastly, the 18 Å resolution EM map of the F_1F_O ATP synthase from *Bos taurus* mitochondria [16•] shows that the bovine peripheral stalk crystal structure, which shares little conservation in sequence and subunit composition to the A/V-type peripheral stalks, needs to be bent in a similar direction to the *Tt*ATPase peripheral stalk structure in order to fit the EM density, indicating that the dynamics of peripheral stalks are a common feature of all rotary ATPase subtypes. Similar to the pushrods in a car, peripheral stalks might be responsible for synchronizing distant parts of rotary ATPases.

Conclusions

Electron microscopy, mass spectrometry and X-ray crystallography are complementary techniques that provide different sets of information to solve molecular 3D puzzles; X-ray crystallography provides high-resolution pictures of subunits akin to the pieces of the puzzle, mass spectrometry provides an inventory list of different types

of pieces and electron microscopy supplies the overall outline of the intact complex.

Improvements in these techniques have provided more complete pictures of all three subtypes of rotary ATPases than ever before, resolving intact complexes to the nanometer scale, giving complete inventory lists of subunits, ligands and lipids that can then be 'puzzled' together to provide models of the complexes as a whole [1]. Additional information from crystal structures in different conformations supported by molecular dynamics provides a revised and more dynamic picture of peripheral stalks, suggesting they are more flexible in one direction than in the other and that their flexibility increases from N-terminus to C-terminus as dictated by their right-handed coiled coil architecture [18••]. This inherent flexibility exactly complements a wobbling motion of the intact rotary ATPase caused by a tilt in between the central axis through the R_1 ring and the central axis through the rotor ring in R_O as observed independently in X-ray structures, EM and single molecule microscopy [18••,47–49]. The concerted movement of all subunits [30,50,51] might increase efficiency, as chemical bonds that stabilize subunit interfaces within the stator remain unchanged. It also suggests novel forms of information transfer within rotary ATPases providing potential mechanisms for regulation and fine-tuning to specific cellular environments. The peripheral stalks thus emerged as key players in information transfer and synchronization of rotary ATPases, in analogy to the pushrods in engines. Interestingly, they also represent the most divergent parts of rotary ATPases both in terms of sequence identity and stoichiometry and provide a simple means for their classification (Figure 1); all known F-type ATPases contain one peripheral stalk, prokaryotic V-type and A-type ATPases contain two and eukaryotic V-type ATPases contain three. The eukaryotic V-type ATPases therefore potentially provide the maximum amount of regulation as the three peripheral stalks connect all three nucleotide-binding subunits with one another and with the ion channel. This is even further enhanced by the large number of organ and organelle specific isoforms of stator subunits and potential post-translational modifications in eukaryotes [33•,52,53]. Future work will undoubtedly provide more detailed insights into the synchronization and regulation of these intricate molecular machines and how the structure and flexibility of individual subunits are choreographed into one unified entity.

Acknowledgements

We would like to thank Chris R. Calladine, Dept. of Engineering, University of Cambridge, UK for stimulating discussions on coiled coil architecture and mechanics.

DS, AGS and MS are funded by Australian National Health & Medical Research Council grants 1004620, 1022143, 1047004, respectively. EML is funded by an Australian Postgraduate Award.

References and recommended reading

Papers of particular interest, published within the period of review, have been highlighted as:

- • of special interest
- •• of outstanding interest

Appendix A. Supplementary data

Supplementary data associated with this article can be found, in the online version, at http://dx.doi.org/10.1016/j.sbi.2013.11.013.

1. Stewart AG, Sobti M, Harvey RP, Stock D: **Rotary ATPases: models, machine elements and technical specifications**. *Bioarchitecture* 2013, **3**:2-12.

2. Iino R, Noji H: **Operation mechanism of F(o) F(1)-adenosine triphosphate synthase revealed by its structure and dynamics**. *IUBMB Life* 2013, **65**:238-246.

3. Forgac M: **Vacuolar ATPases: rotary proton pumps in physiology and pathophysiology**. *Nat Rev Mol Cell Biol* 2007, **8**:917-929.

4. Walker JE: **The ATP synthase: the understood, the uncertain and the unknown**. *Biochem Soc Trans* 2013, **41**:1-16.

5. von Ballmoos C, Cook GM, Dimroth P: **Unique rotary ATP synthase and its biological diversity**. *Annu Rev Biophys* 2008, **37**:43-64.

6. Nakano M, Imamura H, Toei M, Tamakoshi M, Yoshida M, Yokoyama K: **ATP hydrolysis and synthesis of a rotary motor V-ATPase from *Thermus thermophilus***. *J Biol Chem* 2008, **283**:20789-20796.

7. Cross RL, Muller V: **The evolution of A-, F-, and V-type ATP synthases and ATPases: reversals in function and changes in the H+/ATP coupling ratio**. *FEBS Lett* 2004, **576**:1-4.

8. Oster G, Wang H: **ATP synthase: two motors, two fuels**. *Structure* 1999, **7**:R67-R72.

9. Kinosita K Jr, Yasuda R, Noji H, Adachi K: **A rotary molecular motor that can work at near 100% efficiency**. *Philos Trans R Soc Lond B Biol Sci* 2000, **355**:473-489.

10. Watanabe R, Noji H: **Chemomechanical coupling mechanism of F(1)-ATPase: catalysis and torque generation**. *FEBS Lett* 2013, **587**:1030-1035.

11. •• Davies KM, Anselmi C, Wittig I, Faraldo-Gomez JD, Kuhlbrandt W: **Structure of the yeast F1 Fo-ATP synthase dimer and its role in shaping the mitochondrial cristae**. *Proc Natl Acad Sci U S A* 2012, **109**:13602-13607.
ECT of *Saccharomyces cerevisiae* mitochondrial membranes reveals the presence of rows of ATPase dimers. These dimers induce the membrane curvature that forms the mitochondrial cristae.

12. •• Davies KM, Strauss M, Daum B, Kief JH, Osiewacz HD, Rycovska A, Zickermann V, Kuhlbrandt W: **Macromolecular organization of ATP synthase and complex I in whole mitochondria**. *Proc Natl Acad Sci U S A* 2011, **108**:14121-14126.
ECT of mitochondria from different organisms shows ATP synthase dimers are located exclusively at vertices of mitochondrial cristae, while the other respiratory chain complexes are found in adjacent flat sections of the membrane. The authors suggest this allows protons to travel down a concentration gradient, with ATP synthase dimers acting as sinks at the base of the cristae, and this arrangement maximizes the efficieny of ATP synthesis. Interstingly the angle in between dimers varies in different organisms.

13. • Daum B, Walter A, Horst A, Osiewacz HD, Kuhlbrandt W: **Age-dependent dissociation of ATP synthase dimers and loss of inner-membrane cristae in mitochondria**. *Proc Natl Acad Sci USA* 2013, **110**:15301-15306.
ECT of mitochondrial samples taken periodically from *Podospora anserina* as they age demonstrate that ATP synthase dimers dissociate over time. This disrupts the mitochondrial cristae, leading to depolarization of the mitochondrial inner membrane and depletion of cellular ATP levels.

14. •• Lau WC, Rubinstein JL: **Subnanometre-resolution structure of the intact *Thermus thermophilus* H+-driven ATP synthase**. *Nature* 2012, **481**:214-218.

The 9.7 Å resolution EM reconstruction of the *Thermus thermophilus* ATPase is currently the highest resolution structure to be obtained for any intact rotary ATPase. Two bundles of α-helices that can be vizualized in the transmembrane ion channel are proposed to form two half-channels for proton entry and exit, supporting the current model of proton translocation.

15. • Benlekbir S, Bueler SA, Rubinstein JL: **Structure of the vacuolar-type ATPase from *Saccharomyces cerevisiae* at 11-A resolution**. *Nat Struct Mol Biol* 2012, **19**:1356-1362.

This 11 Å resolution EM reconstruction of a V-type ATPase provides evidence for the mechanism by which the V_1 complex is autoinhibited following dissociation, whereby a domain swap in one of the peripheral stalk subunits (subunit H) blocks rotation of the catalytic subunits.

16. • Baker LA, Watt IN, Runswick MJ, Walker JE, Rubinstein JL: **Arrangement of subunits in intact mammalian mitochondrial ATP synthase determined by cryo-EM**. *Proc Natl Acad Sci U S A* 2012, **109**:11675-11680.

The 18 Å resolution EM reconstruction of the bovine F-type ATPase enables vizualization of the interfaces between the ion channel, membrane rotor and membrane-spanning peripheral stalk regions. The structure also provides evidence that the ATP synthase monomer is sufficient to induce membrane curvature.

17. Lee LK, Stewart AG, Donohoe M, Bernal RA, Stock D: **The structure of the peripheral stalk of *Thermus thermophilus* H+-ATPase/synthase**. *Nat Struct Mol Biol* 2010, **17**:373-378.

18. •• Stewart AG, Lee LK, Donohoe M, Chaston JJ, Stock D: **The dynamic stator stalk of rotary ATPases**. *Nat Commun* 2012, **3**:687.

The 2.25 Å crystal structure of the peripheral stalk from the *T. thermophilus* A-type ATPase reveals an inherent flexibility in its right-handed coiled coil architecture. This architecture simultaneously confers rigidity in the direction of rotation to prevent rotation of the catalytic subunits, and provides flexibility in the perpendicular direction to accommodate conformational changes during catalysis.

19. • Oot RA, Huang LS, Berry EA, Wilkens S: **Crystal structure of the yeast vacuolar ATPase heterotrimeric EGC(head) peripheral stalk complex**. *Structure* 2012, **20**:1881-1892.

The structure of the yeast V-type ATPase EGC_{head} complex has been solved in two conformations. It was found that neither conformation, however, fits into the EM density of the intact V-ATPase, indicating the EGC_{head} complex must undergo bending during incorporation into the complex. This bending would induce strain in the peripheral stalks, which the authors have suggested would promote rapid disassembly of the complex, suggesting a regulatory as well as a functional role for the peripheral stalks.

20. Balakrishna AM, Hunke C, Gruber G: **The structure of subunit E of the *Pyrococcus horikoshii* OT3 A-ATP synthase gives insight into the elasticity of the peripheral stalk**. *J Mol Biol* 2012, **420**:155-163.

21. Junge W, Lill H, Engelbrecht S: **ATP synthase: an electrochemical transducer with rotatory mechanics**. *Trends Biochem Sci* 1997, **22**:420-423.

22. Vik SB, Antonio BJ: **A mechanism of proton translocation by F1F0 ATP synthases suggested by double mutants of the a subunit**. *J Biol Chem* 1994, **269**:30364-30369.

23. Watanabe R, Tabata KV, Iino R, Ueno H, Iwamoto M, Oiki S, Noji H: **Biased Brownian stepping rotation of FoF1-ATP synthase driven by proton motive force**. *Nat Commun* 2013, **4**:1631.

24. Fillingame RH: **Subunit c of F1F0 ATP synthase: structure and role in transmembrane energy transduction**. *Biochim Biophys Acta* 1992, **1101**:240-243.

25. Steed PR, Fillingame RH: **Aqueous accessibility to the transmembrane regions of subunit c of the *Escherichia coli* F1F0 ATP synthase**. *J Biol Chem* 2009, **284**:23243-23250.

26. Toei M, Toei S, Forgac M: **Definition of membrane topology and identification of residues important for transport in subunit a of the vacuolar ATPase**. *J Biol Chem* 2011, **286**:35176-35186.

27. • Hakulinen JK, Klyszejko AL, Hoffmann J, Eckhardt-Strelau L, Brutschy B, Vonck J, Meier T: **Structural study on the architecture of the bacterial ATP synthase Fo motor**. *Proc Natl Acad Sci U S A* 2012, **109**:E2050-E2056.

A 7 Å projection map generated by EM of two-dimensional crystals of the F_O rotor from the *Ilyobacter tartaricus* Na^+-translocating ATPase. A four-helix bundle can be vizualized in the ion channel subunit adjacent to the membrane rotor, which is proposed to form part of the ion channel.

28. Pogoryelov D, Krah A, Langer JD, Yildiz O, Faraldo-Gomez JD, Meier T: **Microscopic rotary mechanism of ion translocation in the F(0) complex of ATP synthases**. *Nat Chem Biol* 2010, **6**:891-899.

29. Mizutani K, Yamamoto M, Suzuki K, Yamato I, Kakinuma Y, Shirouzu M, Walker JE, Yokoyama S, Iwata S, Murata T: **Structure of the rotor ring modified with N,N′-dicyclohexylcarbodiimide of the Na(+)-transporting vacuolar ATPase**. *Proc Natl Acad Sci U S A* 2011, **108**:13474-13479.

30. Saroussi S, Schushan M, Ben-Tal N, Junge W, Nelson N: **Structure and flexibility of the C-ring in the electromotor of rotary F(o)F(1)-ATPase of pea chloroplasts**. *PLoS ONE* 2012, **7**:e43045.

31. Symersky J, Pagadala V, Osowski D, Krah A, Meier T, Faraldo-Gomez JD, Mueller DM: **Structure of the c(10) ring of the yeast mitochondrial ATP synthase in the open conformation**. *Nat Struct Mol Biol* 2012, **19**:485-491 S481.

32. •• Zhou M, Morgner N, Barrera NP, Politis A, Isaacson SC, Matak-Vinkovic D, Murata T, Bernal RA, Stock D, Robinson CV: **Mass spectrometry of intact V-type ATPases reveals bound lipids and the effects of nucleotide binding**. *Science* 2011, **334**:380-385.

MS analyses of intact ATPases from *T. thermophilus* and *E. hirae* give insight into subunit stoichiometries and dissociation dynamics of the complexes. These spectra also identify lipids and nucleotides bound to the membrane-embedded subunits, which are proposed to perform regulatory functions within the complex.

33. • Schmidt C, Zhou M, Marriott H, Morgner N, Politis A, Robinson CV: **Comparative cross-linking and mass spectrometry of an intact F-type ATPase suggest a role for phosphorylation**. *Nat Commun* 2013, **4**:1985.

MS of the F-type ATPase from spinach chloroplasts reveals a number of different post-translational modifications within its subunits. Chemical cross-linking experiments of native and phosphatase-treated enzymes demonstrate there are fewer interactions between subunits in the dephosphorylated enzyme, and lower nucleotide occupation at the catalytic sites. This suggests that phosphorylation may mediate interactions between subunits throughout the complex, particularly at the α/β interface, thereby regulating nucleotide binding and stability of the ATPase.

34. Habersetzer J, Ziani W, Larrieu I, Stines-Chaumeil C, Giraud MF, Brethes D, Dautant A, Paumard P: **ATP synthase oligomerization: from the enzyme models to the mitochondrial morphology**. *Int J Biochem Cell Biol* 2013, **45**:99-105.

35. Chaban Y, Boekema EJ, Dudkina NV: **Structures of mitochondrial oxidative phosphorylation supercomplexes and mechanisms for their stabilisation**. *Biochim Biophys Acta-Bioenergetics* 2013. 10.1016/j.bbabio.2013.10.004.

36. Seelert H, Dani DN, Dante S, Hauss T, Krause F, Schafer E, Frenzel M, Poetsch A, Rexroth S, Schwassmann HJ *et al.*: **From protons to OXPHOS supercomplexes and Alzheimer's disease: structure–dynamics–function relationships of energy-transducing membranes**. *Biochim Biophys Acta-Bioenergetics* 2009, **1787**:657-671.

37. Strauss M, Hofhaus G, Schroder RR, Kuhlbrandt W: **Dimer ribbons of ATP synthase shape the inner mitochondrial membrane**. *EMBO J* 2008, **27**:1154-1160.

38. Watt IN, Montgomery MG, Runswick MJ, Leslie AG, Walker JE: **Bioenergetic cost of making an adenosine triphosphate molecule in animal mitochondria**. *Proc Natl Acad Sci U S A* 2010, **107**:16823-16827.

39. Stock D, Leslie AG, Walker JE: **Molecular architecture of the rotary motor in ATP synthase**. *Science* 1999, **286**:1700-1705.

40. Pogoryelov D, Yu J, Meier T, Vonck J, Dimroth P, Muller DJ: **The c15 ring of the *Spirulina platensis* F-ATP synthase: F1/F0 symmetry mismatch is not obligatory**. *EMBO Rep* 2005, **6**:1040-1044.

41. Preiss L, Klyszejko AL, Hicks DB, Liu J, Fackelmayer OJ, Yildiz O, Krulwich TA, Meier T: **The c-ring stoichiometry of ATP synthase**

is adapted to cell physiological requirements of alkaliphilic *Bacillus pseudofirmus* OF4. *Proc Natl Acad Sci U S A* 2013, **110**:7874-7879.

42. Pogoryelov D, Klyszejko AL, Krasnoselska GO, Heller EM, Leone V, Langer JD, Vonck J, Muller DJ, Faraldo-Gomez JD, Meier T: **Engineering rotor ring stoichiometries in the ATP synthase**. *Proc Natl Acad Sci U S A* 2012, **109**:E1599-E1608.

43. • Giorgio V, von Stockum S, Antoniel M, Fabbro A, Fogolari F, Forte M, Glick GD, Petronilli V, Zoratti M, Szabo I *et al.*: **Dimers of mitochondrial ATP synthase form the permeability transition pore**. *Proc Natl Acad Sci USA* 2013, **110**:5887-5892.
ATPase dimers reconstituted into lipid bilayers show sensitivity to cyclophilin D and benzodiazepene 423, leading to the release of mitochondrial matrix Ca^{2+} stores. These have all previously been reported to be properties of the mitochondrial permeability transition pore (PTP), leading the authors to propose the PTP is composed of ATP synthase dimers.

44. Muench SP, Huss M, Song CF, Phillips C, Wieczorek H, Trinick J, Harrison MA: **Cryo-electron microscopy of the vacuolar atpase motor reveals its mechanical and regulatory complexity**. *J Mol Biol* 2009, **386**:989-999.

45. Muench SP, Scheres SH, Huss M, Phillips C, Vitavska O, Wieczorek H, Trinick J, Harrison MA: **Subunit positioning and stator filament stiffness in regulation and power transmission in the V motor of the Manduca sexta V-ATPase**. *J Mol Biol* 2013 http://dx.doi.org/10.1016/j.jmb.2013.09.018.

46. Stewart AG: **The molecular V brake**. *J Mol Biol* 2013 http://dx.doi.org/10.1016/j.jmb.2013.10.003.

47. Sugawa M, Okada KA, Masaike T, Nishizaka T: **A change in the radius of rotation of F1-ATPase indicates a tilting motion of the central shaft**. *Biophys J* 2011, **101**:2201-2206.

48. Giraud MF, Paumard P, Sanchez C, Brethes D, Velours J, Dautant A: **Rotor architecture in the yeast and bovine F(1)-c-ring complexes of F-ATP synthase**. *J Struct Biol* 2011 http://dx.doi.org/10.1016/j.jsb.2011.10.015.

49. Ernst S, Duser MG, Zarrabi N, Dunn SD, Borsch M: **Elastic deformations of the rotary double motor of single F(o)F(1)-ATP synthases detected in real time by Forster resonance energy transfer**. *Biochim Biophys Acta* 2012, **1817**:1722-1731.

50. Moore KJ, Fillingame RH: **Obstruction of transmembrane helical movements in subunit a blocks proton pumping by F1Fo ATP synthase**. *J Biol Chem* 2013, **288**:25535-25541.

51. Sielaff H, Borsch M: **Twisting and subunit rotation in single F(O)(F1)-ATP synthase**. *Philos Trans R Soc Lond B Biol Sci* 2013, **368**:20120024.

52. Futai M, Nakanishi-Matsui M, Okamoto H, Sekiya M, Nakamoto RK: **Rotational catalysis in proton pumping ATPases: from *E. coli* F-ATPase to mammalian V-ATPase**. *Biochim Biophys Acta* 2012, **1817**:1711-1721.

53. Hosokawa H, Dip PV, Merkulova M, Bakulina A, Zhuang Z, Khatri A, Jian X, Keating SM, Bueler SA, Rubinstein JL *et al.*: **The N termini of a-subunit isoforms are involved in signaling between vacuolar H+-ATPase (V-ATPase) and cytohesin-2**. *J Biol Chem* 2013, **288**:5896-5913.

54. Srinivasan S, Vyas NK, Baker ML, Quiocho FA: **Crystal structure of the cytoplasmic N-terminal domain of subunit I, a homolog of subunit a, of V-ATPase**. *J Mol Biol* 2011, **412**:14-21.

55. Rastogi VK, Girvin ME: **Structural changes linked to proton translocation by subunit c of the ATP synthase**. *Nature* 1999, **402**:263-268.

56. Walker JE: **ATP synthesis by rotary catalysis**. *Angew Chem* 1998, **37**:2308-2319.